JOURNAL OF BACTERIOLOGY, Dec. 2007, p. 8564–8574 Vol. 189, No. 23
0021-9193/07/$08.00+0 doi:10.1128/JB.01121-07

Rhodobacter capsulatus OlsA Is a Bifunctional Enyzme Active in both Ornithine Lipid and Phosphatidic Acid Biosynthesis▽†

Semra Aygun-Sunar,[1,2] Rahmi Bilaloglu,[2] Howard Goldfine,[3] and Fevzi Daldal[1]*

Department of Biology, University of Pennsylvania, Philadelphia, Pennsylvania 19104[1]; Department of Biology, Faculty of Art and Sciences, Uludag University, Bursa 16059, Turkey[2]; and Department of Microbiology, School of Medicine, University of Pennsylvania, Philadelphia, Pennsylvania 19104[3]

Received 16 July 2007/Accepted 24 September 2007

The *Rhodobacter capsulatus* genome contains three genes (*olsA* [*plsC138*], *plsC316*, and *plsC3498*) that are annotated as lysophosphatidic acid (1-acyl-*sn*-glycerol-3-phosphate) acyltransferase (AGPAT). Of these genes, *olsA* was previously shown to be an *O*-acyltransferase in the second step of ornithine lipid biosynthesis, which is important for optimal steady-state levels of *c*-type cytochromes (S. Aygun-Sunar, S. Mandaci, H.-G. Koch, I. V. J. Murray, H. Goldfine, and F. Daldal. Mol. Microbiol. 61:418–435, 2006). The roles of the remaining *plsC316* and *plsC3498* genes remained unknown. In this work, these genes were cloned, and chromosomal insertion-deletion mutations inactivating them were obtained to define their function. Characterization of these mutants indicated that, unlike the *Escherichia coli plsC*, neither *plsC316* nor *plsC3498* was essential in *R. capsulatus*. In contrast, no *plsC316 olsA* double mutant could be isolated, indicating that an intact copy of either *olsA* or *plsC316* was required for *R. capsulatus* growth under the conditions tested. Compared to OlsA null mutants, PlsC316 null mutants contained ornithine lipid and had no *c*-type cytochrome-related phenotype. However, they exhibited slight growth impairment and highly altered total fatty acid and phospholipid profiles. Heterologous expression in an *E. coli plsC*(Ts) mutant of either *R. capsulatus plsC316* or *olsA* gene products supported growth at a nonpermissive temperature, exhibited AGPAT activity in vitro, and restored phosphatidic acid biosynthesis. The more vigorous AGPAT activity displayed by PlsC316 suggested that *plsC316* encodes the main AGPAT required for glycerophospholipid synthesis in *R. capsulatus*, while *olsA* acts as an alternative AGPAT that is specific for ornithine lipid synthesis. This study therefore revealed for the first time that some OlsA enzymes, like the enzyme of *R. capsulatus*, are bifunctional and involved in both membrane ornithine lipid and glycerophospholipid biosynthesis.

In many organisms, phosphatidic acid (PA) is a key intermediate in de novo synthesis of glycerophospholipids and in signal transduction (9). Two different pathways are known for the formation of PA: the glycerol-3-phosphate (G3P) pathway and the dihydroxyacetone phosphate pathway. Whereas the G3P pathway of PA synthesis is present in prokaryotes, plants, *Saccharomyces cerevisiae*, and mammalian cells, the dihydroxyacetone phosphate pathway seems to be restricted to yeast and mammalian cells (2). In the G3P pathway, PA is synthesized by two sequential acylation reactions of G3P. In some bacteria like *Escherichia coli*, the first step is catalyzed by the membrane-bound G3P acyltransferase (*sn*-G3P acyltransferase [GPAT]) encoded by *plsB*. GPAT transfers a fatty acyl chain from either acyl-coenzyme A (acyl-CoA) or acyl-acyl carrier protein (acyl-ACP) to the *sn*-1 position of G3P to produce lysophosphatidic acid (LPA) (13, 38) (Fig. 1A, step 1). GPAT is not a widespread enzyme as many bacteria lack a *plsB* homologue and, instead, use the recently identified two-step (PlsX/PlsY) pathway to form LPA (33). In this route, the acyl-phosphate intermediate derived from acyl-ACP by PlsX is transferred to G3P by PlsY to produce LPA (Fig. 1A, step 2). The second step of the G3P pathway is well conserved among bacteria and is catalyzed by an LPA acyltransferase (1-acyl-*sn*-G3P acyltransferase [AGPAT]) enzyme, encoded by *plsC*. In this step, AGPAT acylates the *sn*-2 hydroxyl group of LPA to generate PA (Fig. 1A) (2, 11, 12, 17, 38), which is subsequently converted via the central intermediate CDP-diacylglycerol to membrane glycerophospholipids such as phosphatidylethanolamine (PE), phosphatidylglycerol (PG), and cardiolipin (2). In addition to playing a vital role in phospholipid synthesis, AGPATs are also involved in cell signaling pathways and apoptosis in certain eukaryotic tumor cells (5).

Several membrane-associated AGPATs have been cloned and expressed from many bacteria, yeast, various plant species, and several mammals (6, 7, 8, 12, 14, 22, 27, 29, 37, 42, 44, 45, 49). The well-studied bacterium *E. coli* possesses only one AGPAT, and a deficiency in this enzyme is lethal, resulting in the accumulation of the LPA intermediate (11, 12). Thus, *E. coli plsC* mutants are temperature-sensitive and can be complemented for growth by heterologous expression of plant and mammalian AGPAT homologues (7, 22, 49). Unlike *E. coli*, certain bacteria such as *Neisseria meningitidis*, *Neisseria gonorrhoeae*, *Pseudomonas fluorescens*, and *Pseudomonas aeruginosa* have multiple functional *plsC* homologues that function in diverse environments (4, 14, 42, 45). Multiple AGPAT isozymes expressed in different tissues have been identified in eukaryotes, such as *Limnanthes douglasii*, *Arabidopsis thaliana*,

* Corresponding author. Mailing address: Department of Biology, University of Pennsylvania, 433 S. University Ave., Philadelphia, PA 19104. Phone: (215) 898-4394. Fax: (215) 898-8780. E-mail: fdaldal@sas.upenn.edu.

† Supplemental material for this article may be found at http://jb.asm.org/.

▽ Published ahead of print on 5 October 2007.

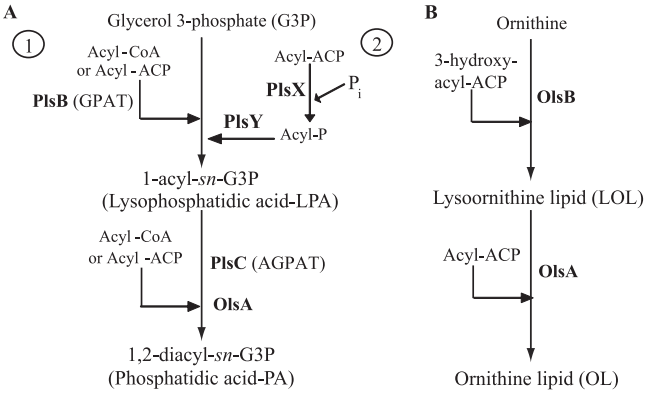

FIG. 1. PA and OL biosynthesis pathway in bacteria. (A) The first step for PA biosynthesis from G3P can be carried out by two different routes. In some bacteria, like *E. coli*, GPAT (PlsB) acylates the *sn*-1 position of G3P using either acyl-ACP or acyl-CoA to form LPA (step 1). In other bacteria, a recently identified route uses the soluble PlsX to convert acyl-ACP to acyl-phosphate (acyl-P), followed by the membrane-associated PlsY transferring the acyl chain to G3P (step 2). In all bacteria, the second step for PA biosynthesis is catalyzed by the membrane-associated AGPAT (PlsC) enzyme, which transfers an acyl chain from either acyl-ACP or acyl-CoA to LPA to yield PA. In *R. capsulatus* OlsA is alternative AGPAT enzyme for production of PA. (B) During OL biosynthesis, the first enzyme OlsB catalyzes the formation of an amide linkage (*N*-acyltransferase) between the α-amino group of ornithine and the carboxyl group of a 3-hydoxy fatty acid, forming LOL. The second enzyme, OlsA, catalyzes the formation of an ester linkage (*O*-acyltransferase) between the 3-hydroxy group of the fatty acyl group and the carboxyl of a second fatty acid, converting LOL to OL.

human, and mouse as well (1, 8, 20, 26, 31, 32, 44, 49, 50). In bacteria, the AGPATs also play a role in regulating lipid acyl composition through their substrate specificities (14, 42). Inactivation of one of the multiple *plsC* genes often alters fatty acid profiles of phospholipids and their membrane properties (14, 42).

Prior to this study, despite the broad importance of AGPATs, only limited knowledge was available on these enzymes, especially those from photosynthetic purple bacteria, including *Rhodobacter* species (C. Benning, personal communication). Earlier, we had isolated *Rhodobacter capsulatus* mutants that are defective in maintaining optimal steady-state levels of *c*-type cytochromes (cyt) (28). Studies of these mutants led us to the identification of *olsA* and *olsB* genes responsible for the biosynthesis of membrane ornithine lipid (OL) in *R. capsulatus* (3) (Fig. 1B). Initially, *olsA* was misannotated as *plsC138* encoding an AGPAT homologue based on its high degree of similarity to acyl-acyltransferases (http://www.ergo-light.com). Mutants lacking an active *olsA* (or *olsB*) were unable to produce OL, but they contained a full complement of membrane glycerophospholipids, including PE, PG, and phosphatidylcholine (PC) (3). Thus, PA production must be carried out by an unknown enzyme distinct from OlsA. A whole-genome survey revealed that the *R. capsulatus* chromosome contained two additional open reading frames (ORFs), annotated *plsC316* and *plsC3498*, as candidates for an AGPAT enzyme involved in PA biosynthesis. In this work, we demonstrate that the *plsC316* product is specific for only PA and not OL biosynthesis and that *plsC3498* is involved in neither of these two pathways. We also show that the *R. capsulatus olsA* product is a bifunctional *O*-acyltransferase involved in both OL and PA biosynthesis. Furthermore, our findings indicate that while *R. capsulatus plsC316* is likely to encode the primary AGPAT enzyme involved in PA biosynthesis, OL synthesis-specific *olsA* can also act as an alternate AGPAT to ensure glycerophospholipid production.

MATERIALS AND METHODS

Bacterial strains and growth conditions. The bacterial strains and plasmids used are listed in Table 1. *E. coli* strains were grown aerobically in LB medium (35), and *R. capsulatus* strains were grown at 35°C in either minimal medium A (MedA) (43) or enriched (MPYE) medium supplemented with appropriate antibiotics, as described previously (36). The ability of various *R. capsulatus* genes to complement the growth defect of a temperature-sensitive *E. coli* PlsC(Ts) mutant (11) was tested by monitoring growth at 42°C on LB plates supplemented with ampicillin (100 mg/ml) and 0 to 2% L-arabinose, as appropriate. The ability of *R. capsulatus* genes to complement an *E. coli* PlsB$^-$ mutant was tested by monitoring at 37°C the G3P auxotrophy of appropriate derivatives of strain SJ22 (*plsB26 plsX50*) (39) on minimal medium E (35) plates supplemented with L-arabinose (2%), ampicillin (100 mg/ml), and 0.04% G3P, as needed.

Molecular genetic techniques. Standard molecular biological techniques were performed according to Sambrook et al. (40) and Daldal et al. (15). Homology searches and amino acid sequence alignments were done using MacVector (Accelerys, San Diego, CA) and appropriate software programs as described earlier (36).

The *plsC316* gene (annotated RRC00316 on the *R. capsulatus* genome) was cloned by PCR amplification using chromosomal DNA and the primers 5′-AA G**TCTAGA**TTCGGCGCCGCCCGATCAGATGGAAA-3′ and 5′-CACC**GGTA CC**CGCGTTCGACCGAAAAATGCCT-3′ containing the XbaI and KpnI sites (in boldface) at positions 689 bp 5′ upstream and 497 bp 3′ downstream of the start and stop sites of *plsC316*, respectively. The 1.9-kb PCR product thus generated was digested with XbaI and KpnI and cloned into the identical restriction sites of the pBluescript II KS (Stratagene Inc., La Jolla, CA) and to pRK415 (19) (Table 1) to yield pSEM21 and pSEM24, respectively (Table 1). Similarly, the *plsC3498* gene (annotated RRC03498 on the *R. capsulatus* genome) was cloned using genomic DNA as a template and the primers 5′-GGTCAA**TCTAGA**TCA GCAGTTGCGCG-3′ and 5′-AAGATC**GGTACC**AAAGCAGAATCC-3′ containing the XbaI and KpnI sites (in boldface) at positions 54 bp 5′ upstream and 58 bp 3′ downstream of the start and stop sites of *plsC3498*, respectively. The 768-bp PCR product thus obtained was digested with XbaI and KpnI and ligated into the corresponding sites of the pBluescript II KS to generate pDML3 (Table 1).

Construction of mutant alleles of *plsC316* and *plsC3498*. Interposon mutagenesis, using either the Kan^r gene of pMA117 (15) or Gm^r gene of pCHB::Gm^r (K. Zhang and F. Daldal, unpublished data), was performed using the gene transfer agent (GTA) (51), as described earlier (15). First, an insertion-deletion allele of *plsC316* was obtained by replacing the 578-bp Tth111I-RsrII blunt-ended fragment of pSEM21 with a 1.6-kb blunt-ended SalI fragment of pMA117 carrying the Kan^r cartridge to yield pSEM31 (Table 1). Similarly, an insertion allele of *plsC3498* was obtained by ligating the 1.16-kb HindIII and XbaI blunt-ended Gm^r cartridge from pCHB::Gm^r into the unique SmaI site of *plsC3498* carried by pDML3 to yield pDML4 (Table 1). Derivatives of the transferable plasmid pRK415 carrying Δ(*plsC316*::*kan*) and *plsC3498*::*gm* deletion-insertion and insertion alleles of *plsC316* and *plsC3498*, respectively, were constructed by cloning the 2.2-kb blunt-ended BglI fragment of pSEM31 between the HindIII and KpnI sites of pRK415 and the 1.87-kb blunt-ended PshAI and KpnI fragment of pDML4 into the KpnI site of pRK415 to generate pSEM32 and pSEM35, respectively (Table 1). The latter plasmids were conjugated into the GTA overproducer strain Y262, and following appropriate GTA crosses into the wild-type strain MT1131, the single mutants SA11 (*plsC3498*::*gm*) and SA13 [Δ(*plsC316*::*kan*)] (Table 1) were obtained. Similarly, the double mutants SA12 [Δ(*olsA*::*spe*) *plsC3498*::*gm*] and SA14 [Δ(*plsC316*::*kan*) *plsC3498*::*gm*] were obtained by using either SA4 [Δ(*olsA*::*spe*)] (3) or SA13 [Δ(*plsC316*::*kan*)] single mutants instead of the wild-type strain MT1131 (Table 1).

Expression of *olsA*, *plsC316*, and *plsC3498* in *E. coli*. The *olsA* gene was PCR amplified using the plasmid pMRC (28) (Table 1) as a template and the primer pairs olsA-NcoI (5′-GGACGC**CCATGG**CACGACCGATCTGG-3′) and olsA-EcoRI (5′-CTGCGC**GAATTC**CGCGACCGCTGACC-3′) containing the NcoI and EcoRI restriction enzymes sites (in boldface), respectively. The *plsC316* gene was amplified using the plasmid pSEM21 (Table 1) as a template and the primers

TABLE 1. Bacterial strains and plasmids used in this study[a]

Strain or plasmid	Description	Relevant characteristic(s)	Reference or source
Strains			
E. coli			
HB101	F$^-$ Δ(*gpt-proA*)*62 leuB6 supE44 ara-14 galK2 lacY1* Δ(*mcrC-mrr*)*rpsL20 xyl-5 mtl-1 recA13*	Str^r; r_B^- m_B^-	40
TOP10	F$^-$ *mcrA* Δ(*mrr-hsdRMS-mcrBC*) ϕ80*lacZ*Δ*M15* Δ*lacX74 deoR recA1 araD139* Δ(*araA-leu*)*7697 galU galK rpsL endA1 nupG*	Str^r; cloning host	Invitrogen
XL-1 Blue	*recA1endA1 gyrA96 thi-1 hsdR17 supE44 relA1 lac* [F′*proAB lacIqZ*Δ*M15* Tn*10*]	Tet^r; cloning host	Stratagene
SM2-1	*plsC1metC162*::*Tn10 thr-1 ara-14* Δ(*gal-attλ*)*hisG4 rpsL136 xyl-5 mtl-1 lacY1 tsx-78 eda-50 rfbD1 thi-1*	*plsC*(Ts) mutant	11
SJ22	*plsB26plsX50 panD2 zac-220*::Tn*10 glpD3 glpR glpKi relA1 spoT1 pit-10 phoA8 ompF627 fluA22 fadL701*	Auxotrophic for G3P on medium E	39
R. capsulatus			
MT1131	*crtD121* Rif^r	Wild type	28
Y262		GTA overproducer	51
SA4	Δ(*olsA*::*spe*)	Spe^r	3
SA11	*plsC3498*::*gm*	Gm^r	This study
SA12	*plsC3498*::*gm* Δ(*olsA*::*spe*)	Gm^r Spe^r	This study
SA13	Δ(*plsC316*::*kan*)	Kan^r	This study
SA14	*plsC3498*::*gm* Δ(*plsC316*::*kan*)	Gm^r Kan^r	This study
SA15	Δ(*olsA*::*spe*) Δ(*plsC316*::*kan*) harboring intact *olsA* on the plasmid	Spe^r Kan^r Tet^r	This study
SA16	Δ(*olsA*::*spe*) Δ(*plsC316*::*kan*) harboring intact *plsC316* on the plasmid	Spe^r Kan^r Tet^r	This study
Plasmids			
pRK2013	*tra*$^+$ (RK2)	Kan^r; conjugative helper	18
pRK415		Tet^r; broad-host-range vector	19
pBSII	pBluescript II (KS+)	Amp^r	Stratagene
pMA117	ΩKan	Kan^r	15
pCHB::Gm^r		Gm^r Tet^r	K. Zhang and F. Daldal
pBAD/*Myc*-His A		Amp^r; arabinose-inducible vector	Invitrogen
pMRC	6-kb chromosomal EcoRI fragment containing *olsA* in pLAFR1	Tet^r	28
pSEM11	Δ(*olsA*::*spe*)	Tet^r Spe^r	3
pDML1	657-bp PCR product containing *plsC3498* cloned into NcoI-EcoRI sites of pBAD/Myc-HisA	Amp^r	This study
pDML3	768-bp PCR product containing *plsC3498* cloned into XbaI-KpnI sites of pBSII	Amp^r	This study
pDML4	XbaI-HindIII-ΩGm of pCHB::Gm inserted into unique SmaI site of *plsC3498* on pDML3	Amp^r Gm^r	This study
pSEM17	828-bp PCR product containing *olsA* cloned into NcoI-EcoRI sites of pBAD/Myc-HisA	Amp^r	This study
pSEM18	NsiI-cut pSEM17 ligated into PstI-cut pRK415	Tet^r Amp^r	This study
pSEM21	1.9-kb PCR product containing *plsC316* cloned into XbaI-KpnI sites of pBSII	Amp^r	This study
pSEM24	1.9-kb XbaI-KpnI fragment of pSEM21 cloned into XbaI-KpnI sites of pRK415	Tet^r	This study
pSEM25	819-bp PCR product containing *plsC316* cloned into NcoI-SfuI sites of pBAD/Myc-HisA	Amp^r	This study
pSEM26	NsiI-cut pSEM25 ligated into PstI-cut pRK415	Tet^r Amp^r	This study
pSEM27	NsiI-cut pDML1 ligated into PstI-cut pRK415	Tet^r Amp^r	This study
pSEM31	578-bp Tth111I-RrsII fragment of *plsC316* on pSEM21 replaced with SalI-Ωkan of pMA117	Amp^r Kan^r	This study
pSEM32	2.2-kb BglI fragment of pSEM31 ligated to HindIII-KpnI sites of pRK415	Tet^r Kan^r	This study
pSEM35	1,870-bp PshAI-KpnI fragment of pDML4 cloned into KpnI sites of pRK415	Tet^r Gm^r	This study

[a] Abbreviations of antibiotic resistances are as follows: Amp, ampicillin; Gm, gentamicin; Kan, kanamycin; Rif, rifampin; Spe, spectinomycin; Str, streptomycin; Tet, tetracycline.

plsC316-NcoI (5′-ATTCGC**CCATGG**TCGTTTGGCAATAC-3′) and plsC316-SfuI (5′-GGCTGACC**TTCGAA**CCGATCTTCATCAGC-3′) containing the NcoI and SfuI (isochizomer BstBI) restriction enzyme sites (in boldface), respectively. The *plsC3498* gene was amplified using genomic DNA as a template and the primers plsC3498-NcoI (5′-CCGGCG**CCATGG**CGGGGCTGACGCG G-3′) and plsC3498-EcoRI (5′-AGGCC**GAATTC**CGCGCCGCCCCCAGC-3′) containing the NcoI and EcoRI restriction enzymes sites (in boldface), respectively. The PCR products obtained were digested with appropriate restriction enzymes, cloned into the corresponding sites of the expression vector pBAD/*Myc*-His A (Invitrogen Inc., Carlsbad, CA), yielding pSEM17 (*olsA*), pSEM25

(*plsC316*), and pDML1 (*plsC3498*), respectively (Table 1). The resulting plasmids were sequenced to confirm that *olsA*, *plsC316*, and *plsC3498* were in frame with the vector's translation start site and were epitope tagged at their carboxyl termini. Automated DNA sequencing with a BigDye terminator cycle sequencing kit (Applied Biosystems, Inc., Foster City, CA) was used with the primers pBAD-Seq-F (5′-ATGCCATAGCATTTTTATCC-3′) and pBAD-Seq-R (5′-GATTTA ATCTGTATCAGG-3′). Derivatives of the transferable plasmid pRK415 carrying *olsA*, *plsC316*, or *plsC3498* were constructed by cloning the 4.9-kb NsiI fragment of pSEM17, the 4.9-kb NsiI fragment of pSEM25, and 4.8-kb NsiI fragment of pDML1 into the PstI site of pRK415 to generate pSEM18, pSEM26, and pSEM27, respectively. Conjugal transfer of all plasmids from *E. coli* to *R. capsulatus* was carried out as described earlier (18).

Expression of *R. capsulatus plsC* homologues in either *E. coli* or *R. capsulatus*. To monitor the expression of *olsA*, *plsC316*, or *plsC3498*, the plasmids pSEM17 (*olsA*), pSEM25 (*plsC316*), or pDML1 (*plsC3498*), respectively, were transformed into the *E. coli* strain SM2-1 [*plsC*(Ts)] (11). Appropriate derivatives of SM2-1 were grown to an optical density at 600 nm (OD_{600}) of ~0.5, and cultures were induced for 4 h with increasing amounts (0 to 2%) of L-arabinose. In each case 1 ml of cell culture was collected by centrifugation, and the whole-cell pellets were resuspended in 100 μl of 2× sodium dodecyl sulfate-polyacrylamide gel electrophoresis (SDS-PAGE) sample loading buffer and boiled for 4 min. To monitor the expression of *olsA*, *plsC316*, or *plsC3498* in *R. capsulatus*, the plasmids pSEM18 (*olsA*), pSEM26 (*plsC316*), and pSEM27 (*plsC3498*) were conjugated into the mutants SA4 (Δ*olsA*::*spe*), SA13 (Δ*plsC316*::*kan*), and SA11 (*plsC3498*::*gm*), respectively. The resulting transconjugants were grown on MPYE plates with or without 1% L-arabinose for 2 days under aerobic conditions. In each case, two isolated colonies were dispersed in 10 μl of distilled H_2O, centrifuged, and resuspended in 10 μl of sample loading buffer. Cells were lysed by incubation at 35°C for 7 min. *E. coli* and *R. capsulatus* cell extracts were separated using 15% SDS-PAGE (30) and transferred to polyvinylidene difluoride membranes. OlsA, PlsC316, or PlsC3498 produced in *E. coli* was detected using monoclonal anti-Myc1-9E10 antibody (at a dilution of 1:1,000) (Cell Center, University of Pennsylvania) as a primary antibody, and the antigen-antibody complexes were detected with horseradish peroxidase-conjugated sheep anti-mouse antibody (at a 1:2,000 dilution) (GE Healthcare Bio-Sciences, Buckinghamshire, United Kingdom) as a secondary antibody, with diaminobenzidine staining enhanced with $NiCl_2$ (25). Similarly, OlsA, PlsC316, or PlsC3498 produced in *R. capsulatus* was detected using the same anti-Myc1-9E10 primary antibody, except that alkaline phosphatase-conjugated goat anti-mouse antibodies (at a 1:2,000 dilution) (Bio-Rad, Hercules, CA) were used as secondary antibodies with the chromogenic substrate 4-nitroblue tetrazolium–5-bromo-4-cloro-3-indolyl phosphate (Sigma Inc., St. Louis, MO).

Analysis of *c*-type cyt. *R. capsulatus* intracytoplasmic membrane vesicles (chromatophores) were prepared using a French pressure cell as described earlier (3). Membrane proteins (100 μg per lane) were incubated at 37°C for 10 min in the sample loading buffer prior to loading, and after separation by 16.5% (wt/vol) tricine-SDS-PAGE (41), the *c*-type cyt were visualized via their peroxidase activities using tetramethylbenzidine and H_2O_2 (46). cbb_3-Cox (cyt *c* oxidase) activity of *R. capsulatus* mutants was determined by using Nadi staining as previously described (28).

Determination of GPAT and AGPAT activities using purified *E. coli* or *R. capsulatus* membranes. Combined GPAT and AGPAT activities of *E. coli* or *R. capsulatus* strains were measured by using a filter paper disk assay (21). The assay mixture contained 0.1 mM Tris-HCl (pH 7.4), 1 mM dithiothreitol, 0.5 mM G3P, 0.005 μCi of [U-^{14}C]G3P, and 7 μM *cis*-vaccenyl-ACP (see the supplemental material for a description of *cis*-vaccenyl-ACP synthesis) in a reaction volume of 20 μl. This mixture was further supplemented with 5 mM Na_3VO_4 as a phosphatase inhibitor when *R. capsulatus* membranes were used. The enzymatic assay, initiated by the addition of membrane particles (see the supplemental material for a description of membrane particle preparation), was carried out for incubations of 0, 1, 2, 5, 10, 15, and 20 min at 35°C. At each time point, 18.5 μl of the reaction mixture was removed and deposited onto Whatmann 3 MM filter paper. Filter papers were washed for 20 min in 10%, 5%, and 1% ice-cold trichloroacetic acid and then dried; the radioactivity retained was determined using a scintillation counter (Beckman LS-9000; Fullerton, CA). A scaled-up version of the same assay (60-μl reaction mixture with a 5-min incubation at 35°C) was also run to monitor LPA and PA production using thin layer chromatography (TLC). At the end of the incubation period, 2 ml of chloroform:methanol (1:1, vol/vol), 0.19 ml of distilled H_2O, and 1 ml of 0.1N KCl were added to the assay mixture. After vigorous vortexing, samples were centrifuged at 8,000 × *g* for 15 min, the lower chloroform phase containing the lipids was evaporated under a stream of argon, and extracted lipids were dissolved in 100 μl of chloroform. Extracts (7,000 and 2,000 total cpm for *E. coli* and *R. capsulatus* extracts, respectively) were applied to a preheated silica gel G60 TLC plate (EMD Chemicals Inc., Gibbstown, PA) and developed with chloroform:methanol:glacial acetic acid (39:9:3, vol/vol/vol) in one dimension. Radiolabeled lipids were visualized using a phosphorimager (Typhoon 9410; Amersham Biosciences, Arlington Heights, IL) and quantitated with ImageQuant software (Amersham Biosciences). Spots corresponding to LPA and PA were identified based on their comigration with unlabeled LPA and PA standards (Avanti Polar Lipids, Alabaster, AL).

Total lipid and fatty acid analyses. For total lipid analyses, *R. capsulatus* cells were labeled for 24 h in 1 ml of MedA or MPYE medium supplemented with 2 μCi of [1-^{14}C]acetate (60 mCi mmol^{-1} specific activity). Labeled cells were analyzed as described previously (3) by using two-dimensional (2D)-TLC, and radiolabeled (60,000 total cpm) lipids were deposited on heat-activated silica gel G60 plates. Plates were developed with chloroform:methanol:water (14:6:1, vol/vol/vol) and chloroform-methanol-glacial acetic acid (13:5:2, vol/vol/vol) for the first and second dimensions, respectively (16). Radiolabeled lipids were visualized, identified, and quantified as described above. Fatty acid compositions of appropriate *R. capsulatus* strains were determined using approximately 30 mg of wet cell pellets grown in MPYE medium, and fatty acid methyl ester analysis was carried out by MIDI Inc. (Newark, DE).

Chemicals, reagents, and enzymes. Restriction enzymes, oligonucleotide primers, [U-^{14}C]G3P (150 mCi mmol^{-1} specific activity) and [1-^{14}C]acetate (60 mCi mmol^{-1} specific activity) were purchased from New England Biolabs, the Cell Center facility of the University of Pennsylvania, American Radiolabeled Chemicals Inc., and NEN Life Science Products, respectively. ACP was obtained from either Sigma Chemical Co. or Invitrogen Inc. *cis*-Vaccenic acid, G3P, and LPA were from Sigma Chemical Co.; PA was from Avanti Polar Lipids; and DEAE cellulose (DE52) was from Whatmann. All other chemicals were from commercial sources and of highest available purity.

RESULTS

Identification of two additional *plsC* homologues in *R. capsulatus* genome. Our previous work established that OlsA null mutants lack only OL; are not lethal, unlike an *E. coli* PlsC mutant; and still produce adequate levels of PE, PC, and PG (3). These findings indicated that in the absence of *olsA*, *R. capsulatus* must have other means of producing PA, which is an essential intermediate for membrane glycerophospholipid biosynthesis. A survey of the *R. capsulatus* genome (http://www.ergo-light.com) revealed two additional AGPAT candidates in addition to RRC00138, which was initially annotated as *plsC138* but subsequently renamed *olsA*, acting as *O*-acyltransferase engaged in OL synthesis (3). The ORFs RRC00316 (*plsC316*) and RRC03498 (*plsC3498*) were annotated as AGPAT homologues, and, like OlsA, they exhibited high degrees of similarities to the *E. coli* PlsC. They contained a conserved acyltransferase (pfam01553/COG0204) motif and a highly conserved (HX_4D) sequence thought to be common to GPAT and AGPAT enzymes (24) (Fig. 2).

On the *R. capsulatus* chromosome, the two *plsC* homologues are located at different regions distant from each other and from *olsA*. *plsC316* is 819 bp in length, encodes 273 amino acids, and is surrounded by the ORFs RRC00314, RRC00315, RRC00701, and RRC00317, corresponding to *mlcA*, *accA*, *ftsX*, and *ftsE*, respectively; *plsC3498* is 657 bp in length, encodes 219 amino acids, and is surrounded by the ORFs RRC03495, RRC03496, RRC03497, and RRC03498 corresponding to *acoB*, *acoC*, *cdsA*, and *cysE*, respectively (see Fig. S1 in the supplemental material and the legend for a functional description of these genes). Multiple alignments of these ORFs illustrated their similarities to the *E. coli* PlsC and to each other (Fig. 2). For example, *R. capsulatus* OlsA, PlsC316, and PlsC3498 show 18%, 19%, and 19% identity and 24%, 32%, and 26% similarity to the *E. coli* PlsC, respectively. Note

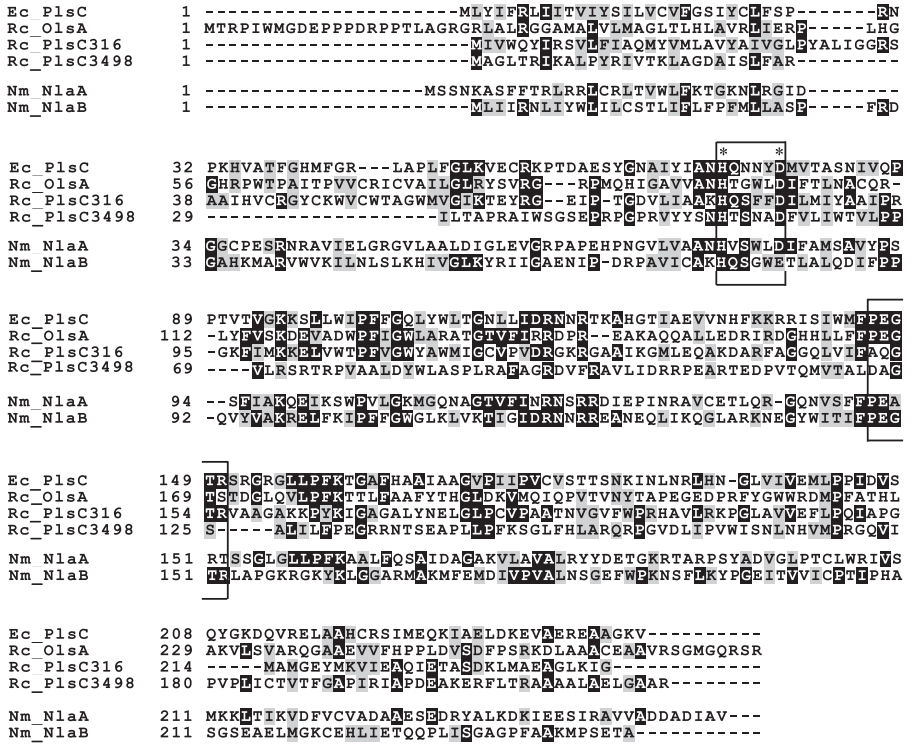

FIG. 2. Comparison of various AGPAT homologues of *R. capsulatus*. The *R. capsulatus* (Rc) AGPAT homologues were aligned with the *E. coli* (Ec) and *N. meningitidis* (Nm) AGPAT sequences using the program ClustalW and presented using the BOXSHADE, version 3.21, software. Identical residues are shaded in black, and similar residues are shaded in gray. The catalytic (HX_4D) motif (24) and the substrate-binding (PEGTR) motif of GPATs and AGPATs are boxed and indicated by asterisks.

that the highest degree of similarity is seen between the *R. capsulatus* PlsC316 and *E. coli* PlsC. Moreover, *plsC316* is also flanked by cell division-related genes *ftsX* and *ftsE* (http://www.ergo-light.com), like the *E. coli plsC* located between *sufI* involved in cell division and *parC* encoding a topoisomerase involved in chromosome partitioning (12). No similar synteny between *E. coli* and *R. capsulatus* was observed for *olsA* or *plsC3498*, which are located immediately downstream of *olsB*, encoding an *N*-acyltransferase involved in OL biosynthesis (3), or *cdsA*, encoding phosphatidate cytidylyltransferase (RRC03497) converting PA to CDP-diacylglycerol, respectively (see Fig. S1 in the supplemental material).

Insertional inactivation of *R. capsulatus plsC* homologues and characterization of ensuing mutants. The *R. capsulatus* AGPAT homologues *plsC316* and *plsC3498* were cloned, and their mutant alleles were constructed using interposon mutagenesis, as described in Materials and Methods, in order to define which one of them is responsible for PA biosynthesis in *R. capsulatus*. The single mutants lacking an active PlsC316 (SA13 [Δ(*plsC316*::*kan*)]) or PlsC3498 (SA11 [*plsC3498*::*gm*]) were obtained readily and compared with a mutant lacking an active OlsA (SA4 [Δ(*olsA*::*spe*)]). Unlike the *E. coli* PlsC$^-$ mutants that are lethal, neither *plsC316* nor *plsC3498* was essential for growth of *R. capsulatus* under the photosynthetic or respiratory conditions on MPYE or MedA growth medium. However, it was noted that the PlsC316$^-$ mutant formed slightly smaller colonies than the OlsA$^-$ or the PlsC3498$^-$ mutants under all growth conditions, indicating a slight growth defect (Fig. 3A). The doubling time of wild-type, OlsA$^-$, and PlsC316$^-$ strains that were grown in liquid MPYE medium were 100, 122, and 131 min, respectively.

Double mutants with all possible combinations of *olsA*, *plsC316*, and *plsC3498* were then sought to probe any possible functional redundancy between these genes. Like the single mutants, the PlsC316$^-$ PlsC3498$^-$ (SA14) and the OlsA$^-$ PlsC3498$^-$ (SA12) double mutants were readily obtained.

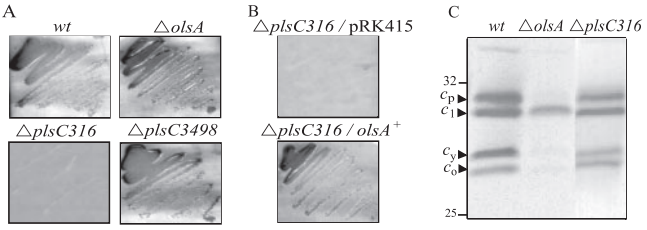

FIG. 3. Characterization of *plsC* mutants. (A) Growth of wild-type (wt), *olsA* (SA4), *plsC316* (SA13), and *plsC3498* (SA11) null mutants on MPYE medium at 35°C under aerobic conditions after 2 days of incubation. (B) Growth of *plsC316* mutant harboring a plasmid with (SA13/pMRC) or without (SA13/pRK415) *olsA* under the same conditions as described for panel A. (C) Comparison of the *c*-type cyt profiles of *R. capsulatus plsC316* and *olsA* mutants. Membrane fractions were isolated from cells grown at 35°C in MPYE medium, proteins were separated by using 16.5% tricine-SDS-PAGE, and the *c*-type cyt were revealed using tetramethylbenzidine, as described in Materials and Methods. The *c*-type cyt subunits of the cbb_3-Cox (c_p and c_o), the cyt bc_1 complex (c_1), and the electron carrier cyt c_y (c_y) are indicated on the left together with the 32.5- and 25-kDa molecular size markers.

These mutants were able to grow on all media tested and exhibited the corresponding single-mutant phenotypes (slow growth and OL deficiency, respectively). Thus, combined inactivation of *plsC316* with *plsC3498* or of *olsA* with *plsC3498* had no deleterious growth effect, indicating that the function of *plsC3498* was not redundant with either of the two other genes. In contrast, despite many attempts under various conditions, inactivation of both *olsA* and *plsC316* was impossible. The inability to obtain an OlsA$^-$ PlsC316$^-$ double mutant strongly suggested that an intact copy of either *olsA* or *plsC316* was required to support growth of *R. capsulatus* under the conditions tested. This observation was further confirmed by using *olsA* or *plsC316* diploid strains (SA15 and SA16) as recipients for interposon mutagenesis (Table 1). These diploid strains carried a copy of a given gene on the chromosome and another copy of the same gene on an autonomously replicating plasmid. Using these strains, mutants carrying inactive chromosomal copies of both *olsA* and *plsC316* but complemented by plasmid-borne copies of either of these genes were readily obtained. The genetic data therefore indicated that an intact copy of either *plsC316* or *olsA* was required for growth of *R. capsulatus*. That OlsA and PlsC316 had overlapping functions was further suggested by the fact that a PlsC316$^-$ mutant regained wild-type-like growth properties when it harbored a plasmid-borne copy of *olsA* (Fig. 3B). However, an OlsA$^-$ mutant carrying an intact copy of *plsC316* was still devoid of OL.

The cyt *c* profiles and membrane polar lipid and fatty acid compositions of *R. capsulatus* mutants lacking various *plsC* homologues. Considering that OL and, hence, its biosynthetic genes *olsA* and *olsB* are required for the presence of normal steady-state amounts of several *c*-type cyt and cbb_3-Cox activity in *R. capsulatus* (3), we examined the effect of *plsC316* inactivation on the *c*-type cyt content of *R. capsulatus*. Analyses of various *plsC316* (Fig. 3C, lane 3) and also *plsC3498* (data not shown) single or double mutants indicated that, unlike OlsA$^-$ mutants, these mutants produced wild-type levels of membrane-bound (Fig. 3C, lane 1) and soluble *c*-type cyt and had cbb_3-Cox activities (data not shown).

Total lipid compositions of the PlsC316$^-$ and PlsC3498$^-$ mutants were next examined after labeling with [1-^{14}C]acetate followed by extraction and 2D-TLC separation, as described in Materials and Methods. The data showed no qualitative differences between the PlsC316$^-$ and PlsC3498$^-$ mutants and the wild-type parental strain MT1131 (Fig. 4). Quantitation of polar lipids was performed using ImageQuant software (Typhoon 9410) (Table 2). Compared with a wild-type strain, inactivation of *plsC316* decreased the relative amounts of PE and increased those of PG and OL, whereas inactivation of *olsA* mainly abolished OL production. Overproduction of OL in the absence of *plsC316* (about 10% versus 4% of total lipids in its presence) suggested that in this mutant OlsA activity might have increased to sustain sufficient PA production, concomitantly leading to higher OL production. On the other hand, absence of *plsC3498* had no affect on the total lipid composition of *R. capsulatus* (data not shown), again suggesting that it was unrelated to membrane lipid biosynthesis.

Total fatty acid profiles of *olsA* or *plsC316* mutants were also compared with the *R. capsulatus* wild-type strain MT1131 by using fatty acid methyl ester analysis, as described in Materials and Methods. The data showed that the fatty acid composition of the membrane lipids was altered in the *olsA* and *plsC316* null mutants (Table 2). In comparison with a wild-type strain, inactivation of *plsC316* decreased and increased modestly the relative amounts of saturated C16 and C18 fatty acids, respectively. Moreover, it drastically decreased the amount of unsaturated C16 but not unsaturated C18 fatty acids. On the other hand, inactivation of *olsA* somewhat increased the amounts of saturated, but not unsaturated, C16 and C18 fatty acids compared to a wild-type strain.

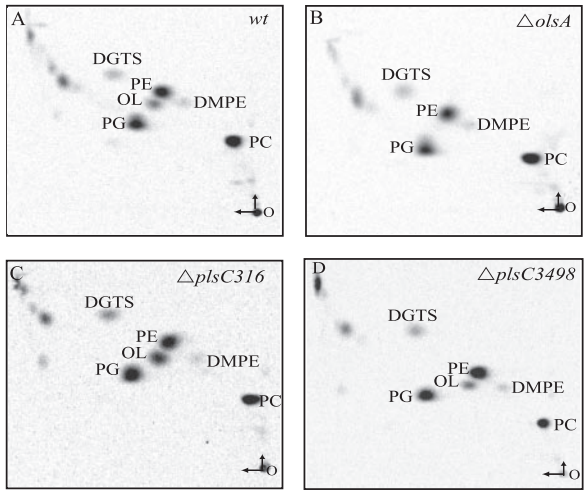

FIG. 4. Total lipid composition of *plsC316* and *plsC3498* null mutants of *R. capsulatus*. In all cases, total polar lipids were extracted from [1-^{14}C]acetate-labeled cells, similar amounts (60,000 cpm) were deposited on TLC plates, and 2D-TLC analyses were carried out as described in Materials and Methods. DGTS, diacylglyceryl trimethylhomoserine; DMPE, phosphatidyl-*N*,*N* dimethylethanolamine. The vertical and horizontal arrows at the origin O refer to the first and second dimension of solvent migrations, respectively. The radioactivity associated with each spot was determined and is given in Table 2.

Both *R. capsulatus olsA* and *plsC316* can complement an *E. coli plsC* mutant in vivo. Pronounced similarities observed between various PlsC homologues (Fig. 2) led us to probe whether any of the *R. capsulatus plsC* homologues could complement the *E. coli plsC*(Ts) mutant, SM2-1, producing a temperature-sensitive AGPAT (12). Plasmid pBAD derivatives, expressing upon induction by L-arabinose either *olsA*, *plsC316*, or *plsC3498*, were constructed as described in Materials and Methods and transformed into the strain SM2-1 at 30°C. Appropriate transformants were tested for their ability to grow at 42°C in the presence of 2% L-arabinose. The plasmid pSEM17 or pSEM25 carrying either *olsA* or *plsC316* was able to complement the *E. coli plsC*(Ts) mutant, SM2-1, for growth at 42°C but only upon induction with L-arabinose (Fig. 5A). Under similar conditions, no complementation was observed with the plasmid pDML1 carrying *plsC3498*. Thus, both OlsA and PlsC316, but not PlsC3498, acted as functional homologues of *E. coli* PlsC and produced apparently temperature-resistant AGPAT activity. Furthermore, it was also noted that *plsC316* provided a more vigorous growth than *olsA*. Immunoblot analyses were carried out to confirm that genetic complementation was due to the production in *E. coli* of *R. capsulatus* OlsA or PlsC316. As expected, upon induction by L-arabinose, α-Myc

TABLE 2. Comparison of polar membrane lipid composition and fatty acid profiles of *R. capsulatus* wild-type, OlsA$^-$, and PlsC316$^-$ mutant strains

Strain	Lipid (%)[b]					Fatty acid (%)						
	PE	PG	PC	OL	Other	$C_{10:0}$ 3OH	$C_{16:0}$	$C_{16:1}\omega7c+C_{16:1}$ $\omega6c$	$C_{18:0}$	$C_{18:0}$ 3OH	$C_{18:1}$ $\omega7c$	$C_{18:1}$ $\omega5c$
Wild type	28.5	18.2	37.7	4.0	11.6	2.60	2.36	6.02	2.09	2.12	79.11	2.98
Δ*olsA* strain	25.7	21.0	44.5	ND	8.9	2.17	5.74	4.14	3.42	1.92	76.91	2.44
Δ*plsC316* strain	16.5	27.9	35.2	10.6	9.7	2.96	1.19	0.59	4.73	2.87	82.39	2.53

[a] All strains were grown on enriched MPYE medium by respiration in the presence of [^{14}C]acetate, and their polar membrane lipids and total fatty acids were analyzed as described in Materials and Methods.
[b] Data are the percentages relative to total ^{14}C. ND, not detected.

epitope-tagged proteins with molecular masses of approximately 31 and 29.5 kDa were detected by using anti α-Myc antibodies in the *E. coli* SM2-1 derivatives harboring OlsA (SM2-1/pSEM17) and PlsC316 (SM2-1/pSEM25), respectively (Fig. 5B, lanes 2 and 4).

Availability of plasmids carrying α-Myc epitope-tagged alleles of OlsA and PlsC316 allowed us to probe whether these proteins were produced in active forms in *R. capsulatus*. The plasmids pSEM18 and pSEM26 carrying *olsA* and *plsC316*, respectively, were crossed into SA4 [Δ(*olsA*::*spe*)] and SA13 [Δ(*plsC316*::*kan*)]. Transconjugants SA4/pSEM18 and SA13/pSEM26 thus obtained were grown in MPYE medium with or without 2% L-arabinose. Immunoblot analyses revealed that they contained proteins of approximately 31 kDa and 29.5 kDa that reacted with anti-Myc antibodies (data not shown). The levels of the proteins produced in *R. capsulatus* were lower than those seen in *E. coli*, but the wild-type phenotypes of the transconjugants in respect to OL, *c*-type cyt production, and better growth indicated that the epitope-tagged versions of OlsA and PlsC316 were functional.

The *E. coli plsB* and *plsC* gene products, conferring GPAT and AGPAT activities, share partial amino acid sequence homologies and are thought to function coordinately (Fig. 1A) (13). Considering that some acyltransferases, like the *Clostridium butyricum plsD* exhibiting functional GPAT activity, can complement an *E. coli* PlsB$^-$ mutant (23) and that *plsC3498* showed similarity to *plsD* (20% identity and 34% similarity), we used the *E. coli* mutant SJ22 to investigate whether *olsA*, *plsC316*, or *plsC3498* exhibited functional GPAT activity. This mutant carries both the *plsB26* and *plsX50* mutations and requires supplementation with G3P for growth (39). Upon transformation of the plasmids pSEM17 (*olsA*), pSEM25 (*plsC316*), and pDML1 (*plsC3498*) into SJ22, no complementation for G3P auxotrophy was observed, indicating that none of these genes produced GPAT activity and especially that *plsC3498* was not a homologue of *plsB* in *R. capsulatus*.

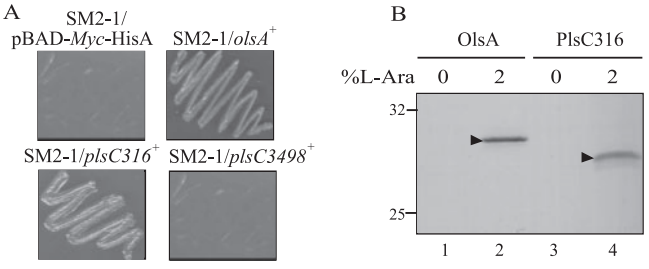

FIG. 5. Expression of *R. capsulatus olsA* and *plsC316* in *E. coli*. (A) The *E. coli plsC*(Ts) strain SM2-1 harboring plasmids carrying *olsA*, *plsC316*, or *plsC3498* of *R. capsulatus* was grown on 2% L-arabinose-containing LB plates at 42°C to score heterologous complementation. SM2-1 cells carrying the cloning vector pBAD/*Myc*-His A were used as a control. (B) Expression of *R. capsulatus olsA* and *plsC316* in *E. coli plsC*(Ts) mutant SM2-1 cells before (0) and after (2) induction with 2% L-arabinose for 4 h at 30°C. Following induction cells were resuspended in 2× SDS loading buffer, and expressed proteins were detected by SDS-PAGE and immunoblotting using anti-Myc antibody as described in Materials and Methods. The triangles point out the *R. capsulatus* OlsA and PlsC316 proteins (31 and 29.5 kDa, respectively) together with the 32.5- and 25-kDa molecular mass markers.

***R. capsulatus* OlsA and PlsC316 exhibit AGPAT activities and synthesize PA in vitro.** In an attempt to define the biochemical function(s) of OlsA and PlsC316, combined GPAT-AGPAT activities were assayed in vitro by using radiolabeled G3P as the acyl acceptor and acyl-ACP as the acyl donor, as described in Materials and Methods. Unlike the *E. coli* GPAT and AGPAT enzymes, which can use either acyl-CoA or acyl-ACP as acyl donors (47), *Rhodobacter sphaeroides* enzymes exhibit high specificity for acyl-ACP compared to acyl-CoA (34). No significant enzyme activity was observed with the acyl-CoA substrate in *R. capsulatus* (data not shown) as in *R. sphaeroides*. Considering that *R. capsulatus* lipids contain predominantly *cis*-vaccenic acid (*cis*-11-18:1) fatty acid, *cis*-vaccenyl-ACP was prepared as the acyl donor. Purified membrane particles (see the supplemental material) from *E. coli plsC*(Ts) mutant SM2-1 derivatives harboring *olsA* or *plsC316* and grown at 42°C in the presence of L-arabinose were assayed. Time course assays monitoring the production of radiolabeled LPA and PA were carried out as described in Materials and Methods. Control experiments established that the activities measured were vaccenyl-ACP and membrane particle dependent (data not shown), and the endogenous activity detected using membranes from SM2-1 cells grown at 30°C and subsequently incubated at 42°C was very low. The data obtained revealed that membranes from SM2-1 derivatives producing either OlsA or PlsC316 exhibited measurable amounts of combined GPAT-AGPAT activity (Fig. 6A). Moreover, PlsC316-containing membrane particles displayed much higher specific activities than either those containing OlsA or those from SM2-1 cells grown at 30°C.

As the combined GPAT-AGPAT assay using radioactive G3P reflects the production of both LPA and PA, separate formation of LPA via GPAT and of PA via AGPAT activities was also determined. Products of a similar enzymatic reaction were analyzed by 1D-TLC, and LPA and PA were identified by comparison of their R_f values with those of standard markers

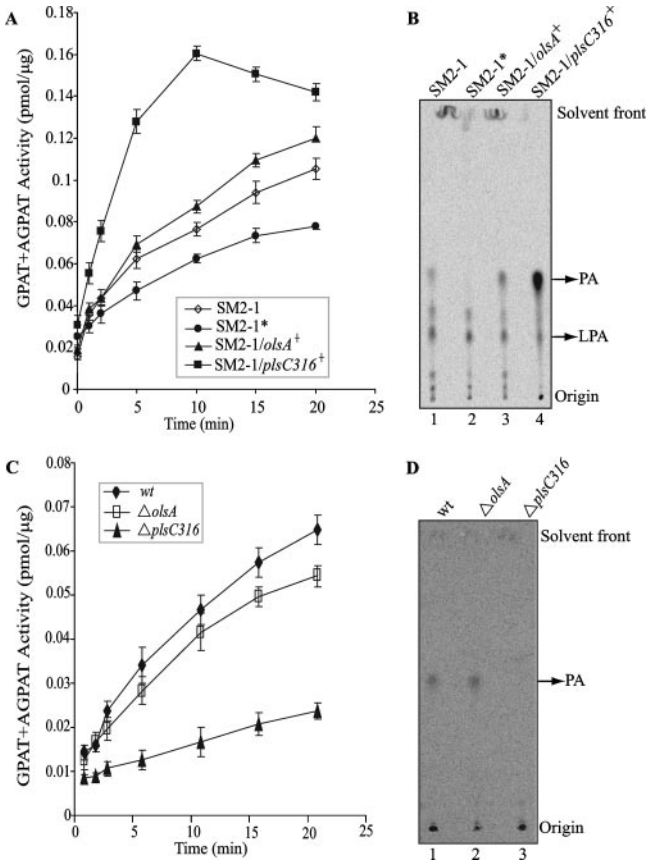

FIG. 6. GPAT-AGPAT activities exhibited by appropriate *E. coli plsC*(Ts) mutants harboring *R. capsulatus plsC* homologues as well as *R. capsulatus* wild-type, *olsA*, and *plsC316* mutants. (A) Time course assays of GPAT-AGPAT activities in *E. coli plsC* mutant harboring *olsA* or *plsC316* were performed using radioactive G3P, vaccenyl-ACP, and membrane particles (prepared as described in the supplemental material) from SM2-1 cells grown at 30°C (SM2-1), SM2-1 cells grown at 30°C with a subsequent 30-min incubation at 42°C (SM2-1*), SM2-1 cells harboring *olsA*, and SM2-1 cells harboring *plsC316*, as described in Materials and Methods. The data shown are the means of two independent experiments with the standard errors, as indicated. (B) Assays similar to those shown in panel A were performed at 35°C for 5 min, and labeled lipids (approximately 7,000 cpm total) were extracted and separated by 1D-TLC, as described in Materials and Methods. LPA and PA produced using membranes from SM2-1 cells grown at 30°C (lane 1), SM2-1 grown at 30°C with a subsequent 30-min incubation at 42°C (lane 2), SM2-1 cells harboring *olsA* (lane 3), and SM2-1 cells harboring *plsC316* (lane 4) are shown. Note the absence of PA production in lane 2 and PA overproduction in lane 4. (C) Time course assays of GPAT-AGPAT activities in wild-type (*wt*), Δ*olsA* (SA4), and Δ*plsC316* (SA13) strains were performed as described for panel A. The data shown are the means of two independent experiments with the standard errors as indicated. (D) Labeled lipids (approximately 2,000 cpm total) were prepared and separated by 1D-TLC, as described for panel B. Note that the PA produced using membranes from the wild-type strain MT1131 and the Δ*olsA* mutant are readily seen while that produced by the Δ*plsC316* mutant is barely detectable.

(Fig. 6B). As expected, all membrane particles produced some amounts of LPA, which reflected the intact GPAT activity of the *E. coli* host SM2-1. On the other hand, membrane particles from heat-treated (42°C for 30 min) SM2-1 cells (grown at 30°C) did not produce any (Fig. 6B, lane 2), whereas those from non-heat-treated cells produced detectable amounts of PA. Similarly, *E. coli* SM2-1 derivatives harboring the *R. capsulatus olsA* or *plsC316* contained AGPAT activity even when grown at 42°C. Moreover, membrane particles harboring PlsC316 or OlsA produced visibly more PA than their parent SM2-1 grown at 30°C (Fig. 6B, lanes 1, 3, and 4). Quantitative estimations using ImageQuant software indicated that the PA production rate was highest (approximately 10 pmol/min/μg of membrane protein) in SM2-1 cells with PlsC316, followed by cells with OlsA (0.875 pmol/min/μg of membrane protein), and lowest in SM2-1 cells grown at 30°C (0.34 pmol/min/μg of membrane protein). Apparently, expression of OlsA or PlsC316 yielded, respectively, approximately 2.5- or 11-fold more PA production than the endogenous activity present in the *E. coli plsC*(Ts) mutant SM2-1 grown at 30°C. We therefore concluded that both *R. capsulatus olsA* and *plsC316* gene products have AGPAT activities, which explained why the presence of either gene was sufficient for membrane glycerophospholipid production and growth of this species. In addition, the vigorous AGPAT activity and the inability to produce OL distinguished PlsC316 from the bifunctional OlsA involved in both PA and OL synthesis and suggested that PlsC316 might be the major enzyme responsible for PA biosynthesis in *R. capsulatus*.

AGPAT activities of *R. capsulatus* PlsC316$^-$ or OlsA$^-$ mutants. Combined GPAT-AGPAT activities in vitro were also determined using membrane preparations from *R. capsulatus* OlsA$^-$ (SA4) or PlsC316$^-$ (SA13) mutants to further establish that PlsC316 is the main enzyme carrying out PA biosynthesis in this species. As expected, the OlsA$^-$ mutant exhibited a combined GPAT-AGPAT activity that was approximately the same as that seen with the wild-type strain MT1131, and the PlsC316$^-$ mutant exhibited much lower (four- to fivefold) GPAT-AGPAT activity relative to both the wild-type strain MT1131 and the OlsA$^-$ mutant SA4 (Fig. 6C). Moreover, TLC with quantitative estimations using ImageQuant software showed that the PA production rate in the OlsA$^-$ mutant was almost identical (approximately 0.8 pmol/min/μg of membrane protein) to that seen with the wild-type strain MT1131 (Fig. 6D, lanes 1 and 2), whereas the PlsC316$^-$ mutant produced barely detectable amounts of PA in vitro (Fig. 6D, lane 3), in agreement with the GPAT-AGPAT activities measured. Therefore, in *R. capsulatus* PlsC316 is apparently the main AGPAT enzyme producing PA for membrane glycerophospholipid synthesis.

DISCUSSION

At the outset of this work, the genes encoding GPAT and AGPAT enzymes were unidentified experimentally in *Rhodobacter* species. Our previous studies on *c*-type cyt biogenesis led us to the identification of the OL biosynthesis genes, *olsA* and *olsB*, of *R. capsulatus* (3) and indicated that the identity of the gene carrying out PA biosynthesis was unclear. The evidence that OlsA$^-$ mutants still produced quasi-normal amounts of PA and glycerophospholipids and the occurrence of at least two additional PlsC homologues on the *R. capsulatus* genome led us to investigate the gene responsible for the AGPAT activity dedicated to PA biosynthesis.

The data obtained in this work indicated that *R. capsulatus plsC3498* is not involved in either PA or OL synthesis.

PlsC3498 shares similarity with both NlaA (15% identity and ~25% similarity) and NlaB (~13% identity and ~28% similarity) from *N. meningitidis*. It possesses the HX_4D sequence thought to correspond to the catalytic motif of GPATs and AGPATs, but compared to OlsA and PlsC316, the substrate binding motif (PEGTR) of AGPATs is not conserved (Fig. 2). It has homology to the *C. butyricum* PlsD (20% identity and 34% similarity), but, unlike PlsD (23), it cannot complement a GPAT-less *E. coli* mutant and does not appear to be a functional homologue of PlsB. Thus, the role of *plsC3498* in *R. capsulatus* remains unknown. Moreover, whether *R. capsulatus* has a true PlsB homologue or whether it utilizes exclusively the PlsX/PlsY pathway for LPA biosynthesis (33) awaits the study of *R. capsulatus* ORFs RRC01510 and RRC02960, which exhibit significant homologies to PlsX (pfam02504/COG0416) (10) and PlsY (pfam02660/COG0344), respectively.

A major outcome of this work were the findings that the gene products of both *olsA* and *plsC316* have AGPAT activities and that *R. capsulatus*, unlike *E. coli*, possesses two AGPAT isozymes capable of producing PA. The AGPAT activities of OlsA and PlsC316 were demonstrated by their ability to complement an *E. coli* mutant that has a temperature-sensitive PlsC and by GPAT-AGPAT activity assays in vitro using membrane particles prepared from appropriate *E. coli* and *R. capsulatus* strains. It was noted that PlsC316 conferred higher AGPAT activities than OlsA but displayed no OL synthesis activity at least in vivo, as $OlsA^-$ mutants are devoid of OL. Moreover, $PlsC316^-$ mutation had no effect on the steady-state amounts of *c*-type cyt, consistent with their OL contents. Thus, our overall findings suggested that PlsC316 is the major AGPAT enzyme, dedicated to PA biosynthesis only. This finding was further supported by the fact that *R. capsulatus* $PlsC316^-$ mutants have much lower AGPAT activities than $OlsA^-$ mutants. On the other hand, OlsA is primarily responsible for OL biosynthesis and also produces some PA to sustain slower growth of *R. capsulatus*. Although OlsA and PlsC316 share homologies with *E. coli* PlsC and act as AGPAT isozymes, they have distinct but overlapping cellular functions. Finally, as double mutants lacking both of these enzymes are lethal, no other gene encoding another functional AGPAT enzyme appears to be present in the *R. capsulatus* genome.

The *O*-acyltransferase OlsA is able to recognize both lyso-ornithine lipid ([LOL] a long-chain acyl amide of ornithine) and LPA (esterified *sn*-G3P) as substrates to which it transfers an acyl group from an acyl-ACP to yield OL and PA, respectively. In both cases, the reaction catalyzed is esterification of an α-CHOH moiety, suggesting broad substrate specificity for this enzyme beyond the accepting group. However, this relaxed substrate recognition does not seem to be a general property of all OlsA enzymes. Apparently, homologues of OlsA from some other bacteria, e.g., *Sinorhizobium meliloti* (48) and *P. fluorescens* (14), do not display any AGPAT activity, as indicated by their inability to complement an *E. coli plsC*(Ts) mutant, unlike the *R. capsulatus* OlsA. Although OlsA enzymes from different species show pronounced similarities to AGPATs of prokaryotes and eukaryotes and contain two conserved domains and the consensus (HX_4D) catalytic motif, it is unclear why some of them are bifunctional and can produce both OL and PA while others can synthesize only OL. A possibility is that different OlsA enzymes might have differing specificities for their acyl donor substrates (acyl-ACP) rather than acyl acceptor substrates (LOL and LPA). If this is the case, then the *R. capsulatus* but not the *S. meliloti* or *P. fluorescens* OlsA seems to recognize *E. coli* ACP efficiently. Also consistent with the more selective behavior of *S. meliloti* OlsA is our earlier observation that *S. meliloti* $OlsA^-$ mutants can be complemented with *R. capsulatus* OlsA but not vice versa (3), suggesting that the latter enzyme has a more relaxed ACP specificity to recognize *S. meliloti* ACP for OL synthesis.

Why some organisms have multiple AGPAT isozymes is interesting. In eukaryotes, the fact that AGPATs are involved in different regulatory circuits with different substrate preferences, like cellular responses to cytokines and growth factors, has been suggested as an explanation the occurrence of multiple AGPATs expressed in different tissues (9, 20, 32). Similarly, some bacterial species including *N. meningitidis*, *N. gonorrhoeae*, and *P. fluorescens* have multiple AGPATs, whereas others, like *E. coli*, appear to have only one such enzyme. It has been suggested that the different isozymes might play different roles, such as fine-tuning the membrane lipid and fatty acid profiles in diverse environments (14, 42, 45). Indeed, while *P. fluorescens* $OlsA^-$ mutants exhibited no major changes in the membrane phospholipid and fatty acid profiles, inactivation of *P. fluorescens* AGPAT isozymes PatB and HdtS did alter the fatty acid profile of phospholipids and some membrane properties (14), as seen here with *R. capsulatus* $OlsA^-$ and $PlsC^-$ mutants.

In the case of *N. meningitidis*, apparently both NlaA and NlaB proteins displayed AGPAT activity in vitro as they complemented a temperature-sensitive *E. coli plsC*(Ts) mutant. Furthermore, this species might have at least an additional enzyme with AGPAT activity as an $NlaA^-$ $NlaB^-$ double mutant is viable and has AGPAT activity (42, 45). Indeed, *R. capsulatus* OlsA and PlsC316 show noteworthy similarities to NlaA (OlsA, ~21% identity and ~32% similarity; PlsC316, ~16% identity and ~30% similarity) and NlaB (OlsA, ~16% identity and 27% similarity; PlsC316, ~26% identity and ~32% similarity), as depicted in Fig. 2. But a closer examination suggests that NlaB seems to be more homologous to PlsC316 and NlaA to OlsA, especially based on the pfam01553/COG0204 motif, suggesting that *N. meningitidis* might contain OL.

In summary, this work demonstrated that of the three *plsC* homologues encountered in the *R. capsulatus* genome, *plsC3498* is not involved in membrane phospholipids or OL biosynthesis. On the other hand, *olsA* and *plsC316* encode efficient AGPAT enzymes able to sustain membrane glycerophospholipid synthesis and growth of *R. capsulatus*; of the two isozymes, PlsC316 seems to be the major enzyme responsible for PA biosynthesis. Finally, the finding that *R. capsulatus* OlsA produces both OL and PA demonstrated for the first time that some OlsA homologues are bifunctional enzymes with overlapping activities. Future studies may shed light on why nature has evolved and conserved multifunctional AGPAT enzymes and how organisms use the specificity and control the promiscuity of these isoenzymes in response to their changing environments.

ACKNOWLEDGMENTS

This work was supported by NIH grants GM38237 (to F.D.) and AI45153 (to H.G.) and Department of Energy grant ER20052 (to F.D.).

We thank Damla Erdogan for help with the constructions of plasmids pDML1, pDML3, and pDML4 and Dong-Woo Lee for assistance with purification of *cis*-vaccenyl-ACP.

REFERENCES

1. **Aguado, B., and R. D. Campbell.** 1998. Characterization of a human lysophosphatidic acid acyltransferase that is encoded by a gene located in the class III region of the human major histocompatibility complex. J. Biol. Chem. **273:**4096–4105.
2. **Athenstaedt, K., and G. Daum.** 1999. Phosphatidic acid, a key intermediate in lipid metabolism. Eur. J. Biochem. **266:**1–16.
3. **Aygun-Sunar, S., S. Mandaci, H.-G. Koch, I. V. J. Murray, H. Goldfine, and F. Daldal.** 2006. Ornithine lipid is required for optimal steady-state amounts of *c*-type cytochromes in *Rhodobacter capsulatus*. Mol. Microbiol. **61:**418–435.
4. **Baysse, C., M. Cullinane, V. Denervaud, E. Burrowes, J. M. Dow, J. P. Morrissey, L. Tam, J. T. Trevors, and F. O'Gara.** 2005. Modulation of quorum sensing in *Pseudomonas aeruginosa* through alteration of membrane properties. Microbiology **151:**2529–2542.
5. **Bonham, L., D. W. Leung, T. White, D. Hollenback, P. Klein, J. Tulinsky, M. Coon, P. De Vries, and J. W. Singer.** 2003. Lysophosphatidic acid acyltransferase-beta: a novel target for induction of tumour cell apoptosis. Expert Opin. Ther. Targets **7:**643–661.
6. **Bourgis, F., J.-C. Kader, P. Barret, M. Renard, D. Robinson, C. Robinson, M. Delseny, and T. J. Roscoe.** 1999. A plastidial lysophosphatidic acid acyltransferase from oilseed rape. Plant Physiol. **120:**913–921.
7. **Brown, A. P., J. Coleman, A. M. Tommey, M. D. Watson, and R. Slabas.** 1994. Isolation and characterisation of a maize cDNA that complements a 1-acyl-*sn*-glycerol-3-phosphate acyltransferase mutant of *Escherichia coli* and encodes a protein which has similarities to other acyltransferases. Plant Mol. Biol. **26:**211–223.
8. **Brown, A. P., C. L. Brough, J. T. Kroon, and J. R. Slabas.** 1995. Identification of a cDNA that encodes a 1-acyl-*sn*-glycerol-3-phosphate acyltransferase from *Limnanthes douglasii*. Plant Mol. Biol. **29:**267–278.
9. **Bursten, S. L., W. E. Harris, K. Bomsztyk, and D. Lovett.** 1991. Interleukin-1 rapidly stimulates lysophosphatidate acyltransferase and phosphatidate phosphohydrolase activities in human mesangial cells. J. Biol. Chem. **266:**20732–20743.
10. **Carty, S. M., A. Colbeau, P. M. Vignais, and T. J. Larson.** 1994. Identification of the *rpmF-plsX-fabH* genes of *Rhodobacter capsulatus*. FEMS Microbiol. Lett. **118:**227–231.
11. **Coleman, J.** 1990. Characterization of *Escherichia coli* cells deficient in 1-acyl-*sn*-glycerol-3 phosphate acyltransferase activity. J. Biol. Chem. **265:**17215–17221.
12. **Coleman, J.** 1992. Characterization of the *Escherichia coli* gene for 1-acyl-*sn*-glycerol-3-phosphate acyltransferase (*plsC*). Mol. Gen. Genet. **232:**295–303.
13. **Cronan, J. E., Jr., and C. O. Rock.** 1987. Biosynthesis of membrane lipids, p. 474–497. *In* F. C. Neidhardt et al. (ed.), *Escherichia coli* and *Salmonella typhimurium*: cellular and molecular biology. American Society for Microbiology, Washington, DC.
14. **Cullinane, M., C. Baysse, J. P. Morrissey, and F. O'Gara.** 2005. Identification of two lysophosphatidic acid acyltransferase genes with overlapping function in *Pseudomonas fluorescens*. Microbiology **151:**3071–3080.
15. **Daldal, F., S. Cheng, J. Applebaum, E. Davidson, and R. C. Prince.** 1986. Cytochrome c_2 is not essential for photosynthetic growth of *Rhodopseudomonas capsulata*. Proc. Natl. Acad. Sci. USA **83:**2012–2016.
16. **de Rudder, K. E. E., J. E. Thomas-Oates, and O. Geiger.** 1997. *Rhizobium meliloti* mutants deficient in phospholipids *N*-methyltransferase still contain phosphatidylcholine. J. Bacteriol. **179:**6921–6928.
17. **Dircks, L., and H. S. Sul.** 1999. Acyltransferases of de novo glycerophospholipid biosynthesis. Prog. Lipid Res. **38:**461–479.
18. **Ditta, G., S. Stanfield, D. Corbin, and D. Helinski.** 1980. Broad host range DNA cloning system for Gram-negative bacteria: construction of a gene bank of *Rhizobium meliloti*. Proc. Natl. Acad. Sci. USA **77:**7347–7351.
19. **Ditta, G., T. Schmidhauser, E. Yacobson, P. Lu, X. Liang, D. R. Finlay, D. Guiney, and D. R. Helinski.** 1985. Plasmids related to the broad host range vector, pRK290, useful for gene cloning and for monitoring expression. Plasmid **13:**149–153.
20. **Eberhardt, C., P. W. Gray, and L. W. Tjoelker.** 1997. Human lysophosphatidic acid acyltransferase. cDNA cloning, expression, and localization to chromosome 9q34.3. J. Biol. Chem. **272:**20299–20305.
21. **Goldfine, H.** 1969. Filter paper disk assay for lipid synthesis. Methods Enzymol. **14:**649–651.
22. **Hanke, C., F. P. Wolter, J. Coleman, G. Peterek, and M. Frentzen.** 1995. A plant acyltransferase involved in triacylglycerol biosynthesis complements an *Escherichia coli sn*-1-acylglycerol-3-phosphate acyltransferase mutant. Eur. J. Biochem. **232:**806–810.
23. **Heath, R. J., H. Goldfine, and C. O. Rock.** 1997. A gene (*plsD*) from *Clostridium butyricum* that functionally substitutes for the *sn*-glycerol-3-phosphate acyltransferase gene (*plsB*) of *Escherichia coli*. J. Bacteriol. **179:**7257–7263.
24. **Heath, R. J., and C. O. Rock.** 1998. A conserved histidine is essential for glycerolipid acyltransferase catalysis. J. Bacteriol. **180:**1425–1430.
25. **Hsu, S. M., and E. Soban.** 1982. Color modification of diaminobenzidine (DAB) precipitation by metallic ions and its application for double immunohistochemistry. J. Histochem. Cytochem. **30:**1079–1082.
26. **Kim, H. U., Y. Li, and A. H. C. Huang.** 2005. Ubiquitous and endoplasmic reticulum-located lysophosphatidyl acyltransferase, LPAT2, is essential for female but not male gametophyte development in *Arabidopsis*. Plant Cell **17:**1073–1089.
27. **Knutzon, D. S., K. D. Lardizabal, J. S. Nelsen, J. L. Bleibaum, H. M. Davies, and J. G. Metz.** 1995. Cloning of a coconut endosperm cDNA encoding a 1-acyl-*sn*-glycerol-3-phosphate acyltransferase that accepts medium-chain-length substrates. Plant Physiol. **109:**999–1006.
28. **Koch, H.-G., O. Hwang, and F. Daldal.** 1998. Isolation and characterization of *Rhodobacter capsulatus* mutants affected in cytochrome cbb_3 oxidase activity. J. Bacteriol. **180:**969–978.
29. **Kume, K., and T. Shimizu.** 1997. cDNA cloning and expression of murine 1-acyl-*sn*-glycerol-3-phosphate acyltransferase. Biochem. Biophys. Res. Commun. **237:**663–666.
30. **Läemmli, U. K.** 1970. Cleavage of structural proteins during the assembly of the head of bacteriophage T4. Nature **227:**680–685.
31. **Li, D., L. Yu, H. Wu, Y. Shan, J. Guo, Y. Dang, Y. Wei, and S. Zhao.** 2003. Cloning and identification of the human LPAAT-zeta gene, a novel member of the lysophosphatidic acid acyltransferase family. J. Hum. Genet. **48:**438–442.
32. **Lu, B., Y. J. Jiang, Y. Zhou, F. Y. Xu, G. M. Hatch, and P. C. Choy.** 2005. Cloning and characterization of murine 1-acyl-*sn*-glycerol-3-phosphate acyltransferases and their regulation by PPARα in murine heart. Biochem. J. **385:**469–477.
33. **Lu, Y., Y. Zhang, K. Grimes, J. Qi, R. Lee, and C. Rock.** 2006. Acylphosphates initiate membrane phospholipid synthesis in gram-positive pathogens. Mol. Cell **23:**765–772.
34. **Lueking, D. R., and H. Goldfine.** 1975. *sn*-Glycerol-3-phosphate acyltransferase activity in particulate preparations from anaerobic, light-grown cells of *Rhodopseudomonas sphaeroides*. J. Biol. Chem. **250:**8530–8535.
35. **Miller, J. H.** 1972. *Experiments in molecular genetics.* Cold Spring Harbor Laboratory, Cold Spring Harbor, NY.
36. **Myllykallio, H., F. E. Jenney, Jr., C. R. Moomaw, C. A. Slaughter, and F. Daldal.** 1997. Cytochrome c_y of *Rhodobacter capsulatus* is attached to the cytoplasmic membrane by an uncleaved signal sequence-like anchor. J. Bacteriol. **179:**2623–2631.
37. **Nagiec, M. M., G. B. Wells, R. L. Lester, and R. C. Dickson.** 1993. A suppressor gene that enables *Saccharomyces cerevisiae* to grow without making sphingolipids encodes a protein that resembles an *Escherichia coli* fatty acyltransferase. J. Biol. Chem. **268:**22156–22163.
38. **Rock, C. O., S. E. Goelz, and J. E. Jr. Cronan.** 1981. Phospholipid synthesis in *Escherichia coli*. Characteristics of fatty acid transfer from acyl-acyl carrier protein to *sn*-glycerol 3-phosphate. J. Biol. Chem. **256:**736–742.
39. **Rock, C. O., and S. Jackowski.** 1982. Regulation of phospholipid synthesis in *Escherichia coli*. Composition of the acyl-acyl carrier protein pool *in vivo*. J. Biol. Chem. **257:**10759–10765.
40. **Sambrook, J., E. F. Fritsch, and T. Maniatis.** 1989. Molecular cloning: a laboratory manual, 2nd. Cold Spring Harbor Laboratory Press, Cold Spring Harbor, NY.
41. **Schägger, H., and G. Von Jagow.** 1987. Tricine-sodium dodecyl sulphate sulfate-polyacrylamide gel electrophoresis for the separation of proteins in the range from 1 to 100 kDa. Anal. Biochem. **166:**368–379.
42. **Shih, G. C., C. M. Kahler, J. S. Swartley, M. M. Rahman, J. Coleman, R. W. Carlson, and D. S. Stevens.** 1999. Multiple lysophosphatidic acid acyltransferases in *Neisseria meningitidis*. Mol. Microbiol. **32:**942–952.
43. **Sistrom, W. R.** 1960. A requirement for sodium in the growth medium of *Rhodopseudomonas sphaeroides*. J. Gen. Microbiol. **22:**77–85.
44. **Stamps, A. C., M. A. Elmore, M. E. Hill, A. A. Makda, and M. J. Finnen.** 1997. A human cDNA sequence with homology to non-mammalian lysophosphatidic acid acyltransferases. Biochem. J. **326:**455–461.
45. **Swartley, J. S., J. T. Balthazar, J. Coleman, W. M. Shafer, and D. S. Stephens.** 1995. Membrane glycerophospholipid biosynthesis in *Neisseria meningitidis* and *Neisseria gonorrhoeae*: identification, characterization, and mutagenesis of a lysophosphatidic acid acyltransferase. Mol. Microbiol. **18:**401–412.
46. **Thomas, P. E., D. Ryan, and W. Levin.** 1976. An improved staining procedure for the detection of the peroxidase activity of cytochrome P-450 on sodium dodecyl sulfate polyacrylamide gels. Anal. Biochem. **75:**168–176.
47. **Van den Bosch, H., and P. R. Vagelos.** 1970. Fatty acyl-CoA and fatty acyl-acyl carrier protein as acyl donors in the synthesis of lysophosphati-

date and phosphatide in *Escherichia coli*. Biochim. Biophys. Acta **218:** 233–248.

48. **Weissenmayer, B., J.-L. Gao, I. M. López-Lara, and O. Geiger.** 2002. Identification of a gene required for the biosynthesis of ornithine-derived lipids. Mol. Microbiol. **45:**721–733.
49. **West, J., C. K. Tompkins, N. Balantac, E. Nudelman, B. Meengs, T. White, S. Bursten, J. Coleman, A. Kumar, J. W. Singer, and D. W. Leung.** 1997. Cloning and expression of two human lysophosphatidic acid acyltransferase cDNAs that enhance cytokine-induced signaling responses in cells. DNA Cell Biol. **16:**691–701.
50. **Ye, G. M., C. Chen, S. Huang, D. D. Han, J. H. Guo, B. Wan, and L. Yu.** 2005. Cloning and characterization a novel human 1-acyl-*sn*-glycerol-3-phosphate acyltransferase gene AGPAT7. DNA Seq. **16:**386–390.
51. **Yen, H. C., N. T. Hu, and B. L. Marrs.** 1979. Characterization of the gene transfer agent made by an overproducer mutant of *Rhodopseudomonas capsulata*. J. Mol. Biol. **131:**157–168.